N-glycosylation in the SERPIN domain of C1-Esterase Inhibitor in hereditary angioedema

Zhen Ren, … , H. Wedner, John P. Atkinson

Research   In-Press Preview   Immunology

Hereditary angioedema is an autosomal dominant disorder caused by defects in C1-esterase inhibitor (C1-INH), resulting in poorly controlled activation of the kallikrein-kinin system and bradykinin overproduction. C1-INH is a heavily glycosylated protein in the serine protease inhibitor (SERPIN) family, yet the role of these glycosylation sites remains unclear. To elucidate the functional impact of N-glycosylation in the SERPIN domain of C1-INH, we engineered four sets consisting of 26 variants at or near the N-linked sequon (NXS/T). Among these, six are reported in HAE patients and five are known C1-INH variants without accessible clinical histories. We systematically evaluated their expression, structure and functional activity with C1‾s, FXIIa and kallikrein. Our findings showed that of the eleven reported variants, seven are deleterious. Deleting N at the three naturally occurring N-linked sequons (N238, N253 and N352) results in pathologic consequences. Altering these sites by substituting N to A disrupts N-linked sugar attachment but preserves protein expression or function. Further, an additional N-linked sugar generated at N272 impairs C1-INH function. These findings highlight the importance of N-linked sequons in modulating the expression and function of C1-INH. Insights gained from identifying the pathological consequences of N-glycan variants should assist in defining more tailored therapy.

Find the latest version:

Title:

N-glycosylation in the SERPIN Domain of the C1-Esterase Inhibitor in Hereditary

Angioedema

Zhen Ren,[1] John Bao,[1] Shuangxia Zhao,[2] Nicola Pozzi,[3] H. Wedner,[1] John P. Atkinson[4]

[1] Department of Medicine, Division of Allergy and Immunology, Washington University School of Medicine, St. Louis, Missouri, USA

[2] Department of Molecular Diagnostics and Endocrinology, The Core Laboratory in Medical Center of Clinical Research, Shanghai Ninth People's Hospital, Shanghai Jiaotong University School of Medicine, Shanghai, China

[3] Department of Biochemistry and Molecular Biology, Edward A. Doisy Research Center, Saint Louis University School of Medicine, St. Louis, MO 63104, USA.

[4] Department of Medicine, Division of Rheumatology, Washington University School of Medicine, St. Louis, Missouri, USA

Correspondence:

Zhen Ren, MD, PhD

Washington University School of Medicine,

660 S Euclid Avenue,

Campus Box 8122, St. Louis, MO 63110, USA

ren.zhen@wustl.edu

Abstract

Hereditary angioedema is an autosomal dominant disorder caused by defects in C1-esterase

inhibitor (C1-INH), resulting in poorly controlled activation of the kallikrein-kinin system and

bradykinin overproduction. C1-INH is a heavily glycosylated protein in the serine protease

inhibitor (SERPIN) family, yet the role of these glycosylation sites remains unclear. To elucidate

the functional impact of N-glycosylation in the SERPIN domain of C1-INH, we engineered four

sets consisting of 26 variants at or near the N-linked sequon (NXS/T). Among these, six are

reported in HAE patients and five are known C1-INH variants without accessible clinical

histories. We systematically evaluated their expression, structure and functional activity with

C1$\bar{\text{s}}$, FXIIa and kallikrein. Our findings showed that of the eleven reported variants, seven are

deleterious. Deleting N at the three naturally occurring N-linked sequons (N238, N253 and

N352) results in pathologic consequences. Altering these sites by substituting N to A disrupts N-

linked sugar attachment but preserves protein expression or function. Further, an additional N-

linked sugar generated at N272 impairs C1-INH function. These findings highlight the

importance of N-linked sequons in modulating the expression and function of C1-INH. Insights

gained from identifying the pathological consequences of N-glycan variants should assist in

defining more tailored therapy.

2

Introduction

Hereditary angioedema (HAE) is an autosomal dominant (AD) disorder caused by defects in the *SERPING1* gene encoding C1-esterase inhibitor (C1-INH) (1). C1-INH is a multi-functional protein that inhibits the contact system, fibrinolytic pathway and complement activation. A dysfunctional C1-INH results in poorly controlled activation of kallikrein-kinin (PKa) system leading to bradykinin (BK) overproduction, known to be the primary mediator of recurrent and unpredictable soft tissue swelling. Laryngeal edema is associated with the risk of asphyxiation, which can be life-threatening (1).

HAE is categorized based on a low laboratory plasma C1-INH antigen level (TY I) or normal antigen but with a dysfunctional C1-INH protein (TY II) (2). This AD disorder results in haploinsufficiency which would be expected to produce 50% of the normal level of C1-INH in plasma (3). However, most patients with HAE present with plasma C1-INH antigen levels of ~ 5 to 30% of normal (4). The cause of these disproportionally decreased C1-INH plasma levels remains largely unknown (5, 6). Further, the severity of clinical symptoms do not necessarily correlate with the antigenic levels of the C1-INH (1).

Over eleven hundred variants in the *SERPING1* gene have been reported and more than one-half are missense SNVs (7). Interpreting the pathogenicity of these *SERPING1* variants can be difficult. This is in part due to the limitations of *in silico* prediction tools and of the genetic variant databases. Relative to the latter, each genetic variant database provides its own unique annotations and datasets, presenting a challenge when integrating clinical and genetic data from different resources.

C1-INH protein contains 500 aa that includes a 22 aa signal peptide, an amino-terminal domain (NTD) consisting of 112 aa and a carboxyl-terminal domain (CTD), also named the serine

79   protease inhibitor (SERPIN) domain, containing 366 aa (Figure 1). The SERPIN domain is

80   highly conserved, comprising 9 α-helices, 3 β-sheets and a reactive center loop (RCL) (Figure

81   2) (8). The target protease binds to the RCL, forming a reversible "Michaelis-Menten complex",

82   and then cleaves the P1–P1′ scissile bond (R466-T467) (9). Upon the cleavage, the SERPIN-

83   protease complex forms a covalent bond between P1 residue of the RCL and the active site

84   serine of the protease (Figures 2-3) (9, 10). The cleaved RCL undergoes drastic conformational

85   changes and inserts into β sheet A (SA), becoming an additional strand, S4A, in the SA domain.

86   This process leads to the formation of an irreversible C1-INH-protease complex (9). In contrast

87   to the well-defined structure and function of the SERPIN domain, the NTD is poorly understood.

88   Crystal structure models of C1-INH are only available for the CTD, as the first one hundred aa

89   from the NTD were not included in the studied structures (Figures 2 and 3) (11).

90

91   In typical glycoproteins, the glycans can constitute up to ~20% of the total weight (12). Whereas

92   C1-INH is a heavily glycosylated protein with an estimated relative electrophoretic mobility (M_r)

93   of 105,000, in which ~ 50% of the mass results from glycosylation (13). C1-INH contains six N-

94   glycosylation sites, of which three sites are in the NTD while the others are in the SERPIN

95   domain (Figure 1 and Figure 3A). The NTD also contains up to 26 O-glycosylation sites (Figure

96   1) (14). Even though most glycans reside in the NTD, the recombinant C1-INH without NTD

97   appears to have preserved SERPIN function, suggesting that N-glycosylation on the SERPIN

98   domain may play a crucial role in stabilizing C1-INH protein, assisting in protein folding, and

99   function (10, 15, 16).

100

101   N-linked glycosylation is the predominant type of glycosylation in eukaryotic cells (17). This

102   process is catalyzed by an oligosaccharyltransferase (OST) through recognition of an N residue

103   in the canonical NXS/T sequon which promotes attachment of a preassembled oligosaccharide

104   to N using an N-glycosidic bond (18, 19). The conserved NXS/T sequon requires an X be at the

105   +1 position, which can be any aa except for P, and either a S or a T at the +2 position of the

106   accepting sequon (18, 19).

107

108   This study investigates the impact of *SERPING1* variants at the N-glycosylation sites in the

109   SERPIN domain. We hypothesized that deleting the N or S/T residue in the NXS/T sequon

110   could destabilize the protein due to it lacking glycosylation modifications. Here, we present a

111   systematic evaluation of four sets of 26 *SERPING1* variants at or near the N-glycosylation sites

112   in the SERPIN domain. Among these, six variants are reported in HAE patients while five

113   variants are known human *SERPING1* variants lacking an accessible clinical history. These

114   studies not only shed new light on the role of N-glycosylation in the SERPIN domain of C1-INH,

115   but also validate how patient variant modeling can help identify pathological consequences and

116   potentially point to improved clinical therapeutic strategies.

117

118   **Results**

119   This study investigates the impact of N-glycosylation on the SERPIN domain of WT C1-INH as

120   well as the effects of known human variants through analysis of four sets of variants either at or

121   near N-glycosylation sites (N238, N253, N352 and N272). Each set of variants includes a N to A

122   substitution, a N deletion and a S deletion at the +2 position of the sequon. In addition, we

123   constructed 11 *SERPING1* variants in close proximity to the N-glycosylation sites based on the

124   published literature, the Genome Aggregation Database V4.1(gnomAD) and the Leiden Open

125   Variation Database V3.0 (LOVD). Among these, six variants are reported in patients with HAE.

126   The variants were expressed recombinantly in human embryonic kidney (HEK) 293T cells

127   containing the intact glycosylation machinery. The protein expression levels of the C1-INH

128   variants were compared to wild-type (WT) C1-INH. We then analyzed the impact of these

129   variants on protein structure and interactions with its functional substrates, including C1s̄, FXIIa

130   and PKa (see Table 1) (21, 22).

131 **N-glycosylation site N238**

132 **Experimental design**

133 The N-glycosylation sequon at N238 employs a consensus sequence, $_{236}$FV**N$_{238}$AS**RTLYSS$_{246}$

134 (Figure 4). To investigate the impact of impaired glycosylation at position N238 on C1-INH

135 expression and function, we created N238A and N238del at the N-linked glycan site and

136 S240del at the +2 position of the sequon. Additionally, we engineered A239D which is reported

137 in gnomAD.

138

139 **Genetic analysis**

140 A239D was reported with an allele frequency (AF) of 0.0004% in the gnomAD and Mastermind

141 databases. This variant has not been reported in other databases, including VarSome, LOVD or

142 ClinVar. *In silico* tools predict this variant to be benign.

143

144 **Structure**

145 N238 is located on the surface of Helix E (hE), which connects strands 1 and 2 of the β-sheet A

146 (S1A and S2A) (Figure 2). The hE plays a crucial role in facilitating the conformation change

147 during the insertion of RCL between S3A and S5A. The deletion of N238 alters the hydrophilic

148 surface of hE and thereby alters the packing of the hE, leading to protein misfolding (Figure 4F).

149

150 **Antigenic and functional analyses**

151 We expressed N238A, N238del, A239D and S240del separately in 293T cells. N238A

152 demonstrates a normal protein secretory pattern while secretion of the recombinantly produced

153 N238del and S240del are barely detectable. The secretion level of A239D is ~ 30% higher than

154 WT (Table 1 and Figure 4A). The binding affinity of N238A and A239D to C1s̄, FXIIa and PKa is

155 comparable to WT (Figure 4, B-E).

156

157 **Implication**

158 The N-linked glycan site at N238 employs an NXS sequon. We hypothesize that deleting the N

159 or S residue likely destabilizes the protein because it lacks proper posttranslational glycan

160 structure modification. In the case of the N238 sequon, the deletion of N or S abolishes protein

161 expression. Replacing N238A leads to normal recombinant protein expression and preserves its

162 function (Figure 4).

163

164 A239D is at the +1 position, 'X' of the NXS sequon, so it can be any aa except P without

165 affecting the recognition of glycan attachment. Compared to WT, A239D exhibits the same M_r

166 and the secretory level of A239D is higher (Table 1 and Figure 4A). A239D demonstrates a

167 normal (comparable to WT) binding affinity to FXIIa and PKa (Figure 4, B-E).

168

169 **N-glycosylation site N352**

170 **Experimental design**

171 The conserved consensus sequence at the N352 position is $_{350}$SH**N$_{352}$LS**LVILVP$_{360}$ (Figure 5A).

172 We constructed N352A, N352del and S354del at the sequon. Based on the data from gnomAD

173 and LOVD, we also created four additional variants: N352I, N352S, L353P and S354G.

174

175 **Genetic analysis**

176 N352S and S354G are reported in gnomAD with an AF of 0.00061% and 0.00065%,

177 respectively. *In silico* predictions for N352S suggest that this change is benign, whereas S354G

178 has conflicting predictions. S345G has a REVEL score of 0.845 and a CADD score of 25.33,

179 indicating a potentially deleterious effect. Other scores, such as pholyP, Pangolin and SpliceAI,

180 indicate that this change is benign. N352I and L353P are reported in an HAE cohort from

181 Germany but are not included in gnomAD (23, 24).

182

183 **Antigenic and Functional Analyses**

184 Variants N352A, N352del, N352I, N352S, L353P, S354del and S354G were individually

185 expressed in 293T cells (Table 1). The secretion of recombinantly produced N352A, N352S and

186 S354G is comparable to WT. The secretion of N352del is markedly decreased, being ~ 10%

187 compared to WT. The secretion of N352I is reduced to ~ 50% compared to WT (Table 1), and

188 L353P and S354del are undetectable. N352I, N352S and S354G show a slightly lower M_r on

189 western blot (WB) compared to WT, ~ 100,000 and 105,000, respectively. Functional analyses

190 reveal that N352A has a normal binding to C1$\bar{s}$, PKa and FXIIa. N352S demonstrates a normal

191 binding to C1$\bar{s}$ and FXIIa but reduced binding to PKa. Both N352I and S354G show mildly

192 reduced binding of FXIIa and PKa, but not to C1$\bar{s}$ (Table 1 and Figure 5, B-E).

193

194 **Structure**

195 N352 is located at the end of loop in the β-sheet 2B (S2B) as it transits into S3B (Figure 5F). It is

196 situated in the center of the breach region, where the RCL inserts into the shutter

197 domain. Deleting N352 destabilizes the packing of S2B and S3B, which may lead to protein

198 misfolding. The replacement of N352 to I is unfavorable. Asparagine (N) is a polar aa and prefers

199 to be on the protein surface. Isoleucine (I) is a hydrophobic aa, which is challenging to adapt to

200 an *α*-helical confirmation and prefers to lie within β-sheets. The substitution of N to I at N352 may

201 change the orientation of the loop, resulting in protein misfolding and thereby leading to a

202 decreased protein expression (Figure 5A). In the case of N352S, both N and S are polar aa.

203 Therefore, substituting N for S is structurally tolerable but alters the glycosylation of N352. S354

204 is located at the tip of the S3B. Replacing a buried S354 with G would markedly reduce the side

205 chain volume. This could cause disruption and alter the packing of the S3B region, thereby

206 leading to C1-INH dysfunction (Figure 5F).

207

208

209 **Implication**

210 The N-linked glycan site at N352 employs an **NLS** sequon and the deletion of N or S in the

211 sequon results in drastically decreased protein expression, which is similar to what we observed

212 at the **N$_{238}$AS** glycosylation site (Table 2). Additionally, replacing N352A led to normal

213 recombinant protein expression, and its functions are preserved. Replacing N352 with both S

214 and I led to a loss of N-linked glycan attachment, resulting in a destabilized protein structure

215 with compromised protein function (Figure 5 and Table 1).

216

217 Recombinant protein L353P is not expressed in 293T cells, which aligns with the prediction that

218 N-glycan can attach in the NXS/T sequon, where X can be any aa except a P. Proline (P)

219 separates the acceptor N from the hydroxyl aa S/T in the sequon and inactivates the acceptor

220 sequence (Figure 5F), forming the structural basis for excluding P residues at the middle

221 position (13, 25).

222

223 **N-glycosylation site N253**

224 **Experimental design**

225 The consensus sequence at the N253 position is $_{251}$LS**N$_{253}$NS**DANLEL$_{261}$ (Figure 6). In this

226 sequon, we engineered N253A and N253del at the N253-glycan site and N254A and N254del

227 at the +1 position N254. Additionally, we introduced S255del, S255G and S255T at the +2

228 position of the sequon.

229

230 **Genetic analysis**

231 S255G is reported in gnomAD with an AF of 0.00014% and *in silico* predictions indicate this

232 change is benign. S255T is reported in LOVD from a HAE patient who also has a frameshift

233 deletion in exon 7 of the *SERPING1* gene (26). This variant has an AF of 0.0027% in gnomAD

234 and *in silico* predictions suggest this missense variant is benign (23, 27). The available

235   evidence is currently insufficient to determine the role of S255T in HAE; therefore, it is

236   categorized as a Variant of Uncertain Significance (VUS).

237

238   **Antigenic and functional analyses**

239   Replacing N253 and N254 with A does not alter recombinant protein expression or secretion

240   (Table 1). Also, deleting N253, N254 and S255 does not affect protein expression (Table 1).

241   Except for variants N254A and S255T, the recombinantly expressed protein from all other

242   variants, including N253A, N253del, N254del, S255del and S255G, migrate at a slightly lower

243   M_r on WB compared to WT, likely due to loss of N-glycan attachment (Figure 6A). After

244   deglycosylation, N254del and S255G run at the same M_r as WT (Figure 6B).

245

246   Our functional analysis indicates that N253A and N254A have normal binding affinities to C1$\bar{s}$,

247   PKa, and FXIIa. N253del and N254del have a decrease in binding to PKa and FXIIa (Figure 6,

248   C-F). However, their binding to C1$\bar{s}$ is normal (Table 1). The binding affinity of S255del, S255G

249   and S255T to PKa, FXIIa and C1$\bar{s}$ is normal (Figure 6, C-F).

250

251   **Structural analysis**

252   N253 and N254 are located at the transition from the loop to hF. The replacement of N to A at

253   N253 and N254 results in a change from hydrophilic N to hydrophobic A, which might alter the

254   packing and orientation of the loop. S255 is located in the beginning section of the hF. Glycine

255   (G) is the smallest aa with only one side chain of hydrogen. Due to its size and being at the

256   transition from loop to hF, the replacement of S255 to G would not interfere with the hF

257   backbone packing (28). In the case of S255T, S and T are both neutral and polar and the

258   change of S to T is structurally tolerable (Table 2) (29).

259

260

261 **Implications**

262 The consensus sequence for the N_{253}**NS** glycosylation site displayed different variant

263 expressions and functional profiles compared to N238 and N352. The deletion of N at the N238

264 or N352 sequons completely abolishes protein expression. Further, the deletion of S240 and

265 S354 at the N_{238}**AS** and N_{352}**LS** sequon, respectively, prevents expression (Figures 4A and 5A).

266 Whereas N253del or N254del in the N_{253}**NS** sequon does not alter the recombinant protein

267 expression but causes a decrease in both PKa and FXIIa binding (Figure 6 and Table 1).

268 Similarly, S255del leads to the loss of the N-glycan site but does not affect the recombinant

269 variant protein expression or function (Figure 6, A and C-F). These changes are likely due to

270 the secondary structure of the N_{253}**NS** sequon in C1-INH. N253 and N254 are at the loop

271 transitioning into hE, whereas S255 resides in the hE. The deletion of N253 or N254 shortens

272 the loop, linking S1A and hE, which leads to a decreased mobility of S1A and hE during RCL

273 insertion. However, the deletion of S255 does not disrupt the hE packing (Figure 6G).

274

275 In the case of S255T, according to the consensus sequence for an N-glycosylation, NXS/T, the

276 replacement of S with T theoretically should not affect the glycol attachment at the N253 site.

277 Our data reveals that the recombinant protein of S255T exhibits the same M_r compared to the

278 WT (Figure 6A), confirming that the replacement of T with S does not affect the N-glycan

279 attachment at the N253 position (27).

280

281 **N-glycosylation site N272**

282 **Experimental design**

283 The sequence at the N272 site is $_{270}$T**NN**$_{272}$**KIS**RLLDS$_{280}$ (Figure 7). K273del is reported in HAE

284 patients and noted to have a higher M_r by creating an additional N-glycosylation site at N272

285 (6). Given that this site contains two Ns, we constructed N271A, N271del, N272A, N272del and

286 S275del. Additionally, we engineered variants N271-N272del and N272D, which are reported

287 by LOVD.

288

Genetic analysis

290 N271-N272del, N272del and K273del are reported in multiple HAE patient studies (5, 30-34).

291 However, these three variants are absent in general population databases (gnomAD). N272D is

292 reported in gnomAD with an AF of 0.0003% and *in silico* analyzes predict that the replacement

293 of N with D is likely benign.

294

Structural analysis

296 K273 is in the loop connecting hF and S3A. Deletion of K273 creates an additional N-

297 glycosylation site on N272 by changing the aa sequence N**N$_{272}$KIS** to an N-glycosylation

298 sequon N**N$_{272}$IS**. Adding an N-glycan at the N272 position reduces the flexibility of the hF/S3A

299 loop, which is critical for the RCL insertion during the transition from an active to a latent state

300 (Figure 7G).

301

Antigenic and functional analyses

303 The secretion of the recombinantly produced variants N271del and N272del is reduced

304 compared to WT (Table 1). The expression levels of variants N271A, N272A, N272D, N271-

305 N272del, K273del and S275del are normal (Figure 7A).

306

307 The variants N271del, N272del and N271-N272del proteins exhibit a decrease in binding to

308 C1$\bar{s}$, FXIIa, and PKa. N271A, N272A and N272D demonstrate normal binding to their

309 substrates compared with WT (Figure 7, C-F). Deleting S275 does not change recombinant

310 protein expression; however, the binding of S275del to PKa is markedly reduced, but not to C1$\bar{s}$

311 or FXIIa. The mechanism of this selective reduction in binding with PKa is under investigation.

312

Implications

A mass spectrometry study reported that the SERPIN domain of C1-INH carries three N-glycosylation sites, N238, N253 and N352 (14). By deleting K273, a glycosylation sequon is created at the N272 position, **NN$_{272}$IS**. The variant protein K273del's binding affinity to C1$\bar{s}$, PKa and FXIIa is reduced secondary to an additional N-linked glycan (Figure 3A) (Table 2).

Discussion

Dysfunctions in C1-INH lead to recurrent and unpredictable episodes of soft tissue swelling in HAE, which can be debilitating and life-threatening. While N-glycosylation can play a key role in stabilizing and folding of proteins, little is known about the role of N-glycosylation in the functionally relevant SERPIN domain of C1-INH. Therefore, we sought to better understand the role of N-glycosylation sites on C1-INH protein expression and function. We strategically evaluated variants at or in close proximity to the three N-linked glycan sequons in the SERPIN domain. Through this study, we determined that the loss of an N-linked sugar at N238, N253 or N352 sites is pathologic (Table 1).

The exact molecular determinants that alter N-glycan co- and posttranslational modifications are unclear (35). OST has two isoforms, STT3A and STT3B, with different roles in mediating N-linked glycosylation. The STT3A isoform is responsible for the cotranslational modification of NXS/T sequon in which the nascent polypeptide enters the lumen of the endoplasmic reticulum (ER). STT3B is mainly responsible for posttranslational N-glycosylation, modifying consensus sites that are not glycosylated by STT3A. The depletion of STT3A, but not STT3B, results in the induction of the unfolded protein response pathway. This pathway involves downregulating the transcription of secretory proteins and increasing the removal of misfolded proteins through ER-associated degradation (36-39).

338

339   In this study, we first addressed if the lack of N-glycosylation alters C1-INH protein production.

340   The deletion of an N residue at $N_{238}AS$ or $N_{352}LS$ results in the abolition of recombinant C1-INH

341   protein expression by 293T cells. Further, C1-INH variants with an S deletion at the +2 position

342   (at these same loci), including S240del and S354del, are also not expressed. Interestingly,

343   N238A and N352A mutants display preserved protein expression and functional levels despite

344   lacking N-glycan attachment.

345

346   These data suggest that N-glycosylation sites at $N_{238}AS$ and $N_{352}LS$ sequons are likely required

347   for cotranslational N-glycan modification. The replacement of N with A at N_{238} and N_{352} sequons

348   is tolerable structurally and these variants could undergo folding and being exported outside of

349   ER. However, errors in protein folding (misfolded protein) due to N and S deletion likely trigger

350   protein cotranslational degradation (Figure 8) (40, 41).

351

352   Unlike the N-glycosylation sites at $N_{238}AS$ and $N_{352}LS$ sequon, the site at $N_{253}NS$ contains two

353   **N**s and exhibits different patterns. When N residues are deleted at the $N_{253}NS$ site, the variants

354   N253del and N254del show normal recombinant protein expression comparable to WT. Further

355   S deletion at the +2 position of $N_{253}NS$ sequon also results in a preserved protein expression

356   comparable to WT. All three mutants migrate at a lower M_r on WB than WT due to a lack of N-

357   linked glycan attachment at N253 (Figure 6).

358

359   The influences of the middle "X" residue in N-glycan sequon, NXS, have been studied. If X is a

360   small, non-charged aa, it can be N-glycosylated in an efficient cotranslational manner. In

361   contrast, consensus sites with bulky hydrophobic, negatively charged middle X residue, in a

362   close spacing between NXS acceptor site or within the cysteine-rich domain, often result in a

363   higher percentage of N-glycans being added vis posttranslational modification (27, 42, 43). We

364   hypothesize that the N-glycosylation at $N_{253}NS$ occurs during posttranslational modification and

365   the deletion of either N is tolerable without disrupting protein structural folding. Therefore, the

366   recombinant protein is synthesized and secreted despite lacking N-glycan modification (Figure

367   6).

368

369   NXS/T sequons are highly conserved in the SERPIN domain of C1-INH. At the $N_{352}XS/T$

370   sequon, variant L353P is not expressed in 293T cells. This is consistent with the prediction that

371   at the X position in the NXS sequon, it can be any aa but not P as it physically prohibits N-linked

372   sugar attachment. Additionally, the consensus NXS sequon indicates that S can be replaced by

373   T or, less often, C. In the case of the $N_{253}NS$ sequon, the variant S255T exhibits a normal

374   protein expression and function (Figure 6), supporting the conservation of the NXS/T sequon.

375

376   N-glycosylation sites N238, N253 and N352 are located on the SERPIN domain of C1-INH and

377   have been confirmed by mass spectrometry (14). N272 glycosylation site is noted in The

378   Complement Factsbook (13). However, this N-glycan location site in human C1-INH has not

379   been verified by mass spectrometry. Our understanding of the impact of glycosylation

380   modifications on C1-INH is currently limited. The recombinant C1-INH produced in the

381   mammary gland of transgenic rabbits is available for treating acute lesions in HAE (44, 45). Due

382   to a lower degree of glycosylation, its efficiency suffers from an extremely short half-life of 2.4-

383   2.7 hrs, compared to human plasma-derived C1-INH, with a half-life of 56-72 hrs (44). A

384   question our study investigated is whether an increased number of glycosylation sites would

385   better facilitate the C1-INH function. This was further "sparked" when we identified two

386   unrelated HAE patients carrying heterozygous *SERPING1* variants affecting neighboring aa,

387   N272 and K273. The patient carrying N272del presented as a TYI HAE laboratory phenotype

388   with a low C1-INH serum level, whereas the patient with K273del demonstrated a TYII

389   phenotype with a normal C1-INH serum level but with dysfunctional C1$\bar{s}$ binding (6). The

390   deletion of K273 created a new N-glycosylation site as **N$_{272}$IS** sequon. The recombinantly

391   expressed K273del protein exhibited an increased M$_r$ compared to WT, likely due to another N-

392   linked glycan attachment (Figure 3A and Figure 7, A and B). Further functional analyses of

393   K273del demonstrated impaired binding activity to C1$\bar{s}$, PKa and FXIIa. The presence of the

394   additional N-linked glycan likely hindered the insertion of RCL between S3A and S5A (Figure 2

395   and Figure 7G). This insight, gained from the additional N-glycan site in the K273del, deepened

396   our understanding of the impact of N-glycosylation sequon on C1-INH protein function and may

397   be valuable for future consideration in protein modification and engineering (6, 46) of N-linked

398   glycosylation sites.

399

400   The growing application of next-generation sequencing (NGS), exome or whole genome

401   sequencing in investigating rare diseases has led to the identification of an increased number of

402   variants in the *SERPING1* gene (47). To date, more than eleven hundred genetic variants are

403   reported, among which about one-third are single nucleotide variants (SNVs) resulting in

404   missense mutations (34, 47). Assessing the pathogenicity of these variants can be challenging

405   as more than one-half of them are classified as a VUS (47).

406

407   In this study, we conducted strategic analyses to examine 11 reported SNVs near the three N-

408   glycan sites in the SERPIN domain. Among these, five variants, A239D, S255G, N272D, N352S

409   and S354G, are reported in gnomAD without an accessible clinical history. The other six

410   variants, S255T, N352I, L353P, N271-N272del, N272del and K273del are reported in HAE

411   patients (Tables 1 and 2). At the N352 glycosylation site, both N352I and L353P are likely

412   pathogenic (Table 2). N352I exhibits markedly decreased protein expression and L353P is not

413   expressed. At the N253 glycosylation site, two variants are likely benign, S255G and S255T,

414   with normal recombinant protein expression and binding affinity to PKa, FXIIa and C1$\bar{s}$ (Figure

415   6C). At the N272 site, K273del has an additional N-glycan site and is dysfunctional and N272del

416   has low protein expression and function. N271-N272del is a rare variant reported in TYI HAE

417   patients from a Macedonian cohort (31). Recombinant protein expression of N271-N272del is

418   normal, but its binding affinity to C1$\bar{s}$, PKa and FXIIa is decreased. N271 and N272 are in the

419   loop connecting hF and S5A, conserved aa in the SERPIN domains (Supplemental Figure 1).

420   The deletion of N271-N272 likely disrupts the packing of S5A/hF and further destabilizes the

421   SERPIN domain folding and function (Figure 7G).

422

423   It is worth noting that variants S275del and N352S show normal protein expression but

424   selectively impair PKa binding. The mechanism of the selectively impaired SERPIN inhibition is

425   not well understood, although it was reported in a study of twelve C1-INH P1 variants (16). The

426   inhibitory activities of twelve R466 variants at the P1 position of RCL in the SERPIN domain

427   were tested with C1$\bar{s}$, FXIIa, PKa and plasmin. Selectively impaired binding activity of

428   P1R466K was observed in FXIIa, less in PKa and not in C1$\bar{s}$ or plasmin (16). Currently, the

429   diagnosis of HAE is based on abnormal complement laboratory studies and genetic testing is

430   not routinely performed. The functional analysis of C1INH is only commercially available to

431   assess its binding to C1$\bar{s}$ but not to other substrates, such as PKa, FXIIa and thrombin. Various

432   HAE therapies are available, including C1INH replacement, PKa inhibitors, FXIIa inhibitors,

433   antifibrinolytics, and B2R antagonists, with a high average cost of $700,000 per patient-year

434   (48). Managing the disease effectively with optimal treatment choices continues to be a

435   persistent challenge. Thus, these findings provide valuable insights for assisting the formulation

436   of personalized treatment by opening up the possibility of selectively choosing a medicine to

437   directly target a specific defect that is impaired in patients with a C1-INH variant.

438

439   This investigation focuses on analyzing the impact of N-glycosylation in the SERPIN domain by

440   examining the expression, structure and function of *SERPING1* variants. The results are most

441   consistent with a pathologic consequence (i.e. HAE) if a missense mutation that alters/deletes

442   an N-linked sugar at four distinct sites in the SERPIN domain of C1-INH protein. Our findings

443   suggest that N238 and N352 glycosylation sites undergo cotranslational modification mediated

444   by the STT3A complex, adding oligosaccharides to the nascent protein during its insertion into

445   the ER. This process is crucial for assisting nascent protein folding and transportation (49)

446   (Figure 8A). The failure of attaching N-glycan to these two sites can lead to protein misfolding

447   and trigger cotranslational protein degradation (Figure 8B) (50). Conversely, we postulate that

448   the N253 glycosylation site is modified through posttranslational modification mediated by the

449   STT3B complex. N253 is in close spacing between at $N_{238}AS$ and $N_{352}LS$ sequons that promote

450   skipping by the STT3A complex. The posttranslational N-glycosylation at N253 is required but

451   not necessary to acquire native protein structure. In the absence of N253-glycan attachment,

452   the effect is tolerable compared to N238 and N352 sites (Figure 8C) (38, 50, 51). N253 site

453   variants have preserved expression levels comparable to WT (Figure 6). In addition, our finding

454   demonstrates that adding an additional N-glycosylation site can be deleterious by interrupting

455   the SERPIN domain function. The scope of this study is limited to only analyzing the N-

456   glycosylation sites on the SERPIN domain. Further research is warranted to understand the

457   structure and function of the N-glycosylation sites on the NTD.

458

459   **Methods**

460   *Sex as a biological variable.* As only 293T cells were used in this study, sex was not considered

461   as a biological variable.

462

463   *Preparation and expression of variants.* The *SERPING1* pcDNA3.1 expression vector

464   (Genescript, NJ, USA) was used to create the C1-INH variants. The variants were produced

465   using the QuikChange XL site-directed mutagenesis kit (Agilent Technologies, Santa Clara,

466   CA). Each *SERPING1* cDNA clone was sequenced. The variants were transient transfected into

467   293T cells (ATCC, CRL-3216) using the Xfect reagent (Takara Bio USA, CA) where Dulbecco's

468   Modified Eagle Medium (DMEM) was replaced with OptiMEM® (Invitrogen, NY). Each

469   transfection experiment was conducted in three independent biological replicates. Supernatants

470   were collected after 48 h, concentrated 40× and then stored in aliquots at -80°C (20).

471

472   *Quantification and Western blotting (WB).* The quantity of each recombinant C1-INH variant

473   protein was determined by ELISA according to the manufacturer's recommendations (Abcam,

474   Cambridge, MA). Electrophoretic patterns were evaluated and compared to WT using

475   transfectant supernatants that were analyzed under reducing conditions using 4-20% SDS-

476   PAGE, transferred to nitrocellulose and then probed with 1:1,000 rabbit anti-human C1-INH

477   mAb (Abcam, AB134918) as the primary antibody, specifically recognizing the NTD of C1-INH

478   between amino acids 22 to 100, followed by a 1:10,000 horseradish peroxidase (HRP)-

479   conjugated goat anti-rabbit IgG (Abcam, AB205718).

480

481   *C1s̄, FXIIa and PKa binding assays*.

482   *C1s̄* . The binding of C1s̄ to C1-INH was measured according to the manufacturer's instruction

483   (Quidel, San Diego, CA). In the first step, standards, controls and C1-INH variants were

484   incubated with biotinylated C1s̄. Next, the incubation mixtures containing the C1-INH-C1s̄

485   complex were added to microtiter wells precoated with streptavidin. After incubation, the wells

486   were washed 3× to remove unbound protein. Then, the goat anti-human C1-INH was added to

487   each test well to bind with the C1-INH-C1s̄ complex captured on the surface of the streptavidin-

488   coated microtiter wells. After washing, the HRP-conjugated goat anti-human Ab was added to

489   each microassay well. The HRP-conjugate reacted with the C1-INH-C1s̄ complex. After adding

490   3, 3', 5, 5'- tetramethylbenzidine dihydrochloride (TMB) substrate, the complex generated a

491   yellow color. The intensity of the color reaction mixture was measured spectrophotometrically at

492   450 nm.

493

494   *FXIIa and PKa.* Purified human FXIIa and PKa were obtained from Enzyme Research

495   Laboratories (South Bend, IN, USA). The biotinylation kit and streptavidin-coated plate were

496   obtained from Thermo Scientific (Rockford, IL, USA). FXIIa and PKa were biotinylated

497   according to the manufacturer's recommendations. In brief, FXIIa and PKa were dissolved in

498   phosphate-buffered saline (PBS) and then incubated with Sulfo-NHS-LC-biotin on ice for 2 h.

499   Excess nonreacted and hydrolyzed biotin was removed through a spin column and the biotin-

500   labeled protein concentrations were measured by NanoDrop. ELISA was utilized to assess the

501   binding of WT and variant C1-INH to FXIIa and PKa, as described previously(21). Biotinylated

502   FXIIa and PKa (25 μl of 2 μg/ml), an equivalent molar amount of C1-INH, and 50 μl of reaction

503   buffer (2% BSA in PBS-T) were added to the streptavidin-coated plate and incubated for 1 h at

504   37° C. The bound PKa-C1-INH or FXIIa-C1-INH complex was detected by 1:10,000 mouse

505   anti-C1-INH mAb (Abcam, Cambridge, MA), followed by incubation at RT for 1 h. After

506   incubation, the plates were washed 3× using PBS-Tween (300 μl/each). A 1:10,000 dilution of

507   HRP-conjugated goat anti-rabbit IgG (Abcam, Cambridge, MA) secondary Ab was added and

508   then incubated at 37° C for 1 h. The detection of bound C1-INH complex was carried out as

509   described previously (21). On at least three occasions, binding assays were performed

510   employing serially diluted samples. C1s̄, FXIIa and PKa binding assays were repeated a

511   minimum of 3× for each variant.

512

513   *Molecular modeling.* PyMOL Version 3.0 was employed to visualize and analyze the

514   protein structures.

515

516 *Data availability.* Values for all data points in graphs are reported in the Supporting Data Values

517 file. All gel data and WBs in this study are presented in the full, unedited gel file available in the

518 Supplemental Data with full annotations.

519

520 *Statistical analyses.* Statistical analyses were performed using Prism 10 (GraphPad, San Diego,

521 USA). Comparisons between two groups were assessed using paired t-test (non-parametric).

522 Comparisons among groups were performed using a 1-way ANOVA with Dunnett's multiple

523 comparison test ($P < 0.05$ was considered as significant). The relative absorbance was

524 calculated as the absorbance for each C1-INH variant divided by the absorbance of WT at

525 protein concentrations of 125 ng/ml, 250 ng/ml, 500 ng/ml and 1 μg/ml.

526

527 **Author contributions:** ZR and JPA conceived and designed the experiments, analyzed the

528 data and interpreted results. ZR and JB performed the experiments. ZR conducted the

529 structural analysis. SZ classified variants in accordance with ACMG 2015 criteria. ZR prepared

530 the figures and drafted the manuscript. ZR, JB, SZ, NP, JW and JPA edited the manuscript.

531

542

543

544

545   **References**

546   1.   Zuraw BL. Clinical practice. Hereditary angioedema. *N Engl J Med.* 2008;359(10):1027-

547   36.

548   2.   Bissler JJ, Aulak KS, Donaldson VH, Rosen FS, Cicardi M, Harrison RA, et al. Molecular

549   defects in hereditary angioneurotic edema. *Proc Assoc Am Physicians.*

550   1997;109(2):164-73.

551   3.   Bock SC, Skriver K, Nielsen E, Thogersen HC, Wiman B, Donaldson VH, et al. Human

552   C1 inhibitor: primary structure, cDNA cloning, and chromosomal localization.

553   *Biochemistry.* 1986;25(15):4292-301.

554   4.   Pappalardo E, Zingale LC, and Cicardi M. C1 inhibitor gene expression in patients with

555   hereditary angioedema: quantitative evaluation by means of real-time RT-PCR. *J Allergy*

556   *Clin Immunol.* 2004;114(3):638-44.

557   5.   Ryo LB, Haslund D, Rovsing AB, Pihl R, Sanrattana W, de Maat S, et al. Restriction of

558   C1-inhibitor activity in hereditary angioedema by dominant-negative effects of disease-

559   associated SERPING1 gene variants. *J Allergy Clin Immunol.* 2023;152(5):1218-36 e9.

560   6.   Ren Z, Zhao S, Li T, Wedner HJ, and Atkinson JP. Insights into the pathogenesis of

561   hereditary angioedema using genetic sequencing and recombinant protein expression

562   analyses. *J Allergy Clin Immunol.* 2023;151(4):1040-9 e5.

563   7.   Guan X, Sheng Y, Liu S, He M, Chen T, and Zhi Y. Epidemiology, economic, and

564   humanistic burden of hereditary angioedema: a systematic review. *Orphanet J Rare Dis.*

565   2024;19(1):256.

566   8.   Dijk M, Holkers J, Voskamp P, Giannetti BM, Waterreus WJ, van Veen HA, et al. How

567   Dextran Sulfate Affects C1-inhibitor Activity: A Model for Polysaccharide Potentiation.

568   *Structure.* 2016;24(12):2182-9.

569   9.   Garrigues RJ, Garrison MP, and Garcia BL. The Crystal Structure of the Michaelis-

570   Menten Complex of C1 Esterase Inhibitor and C1s Reveals Novel Insights into

571   Complement Regulation. *J Immunol.* 2024;213(5):718-29.

572   10.   Davis AE, 3rd, Mejia P, and Lu F. Biological activities of C1 inhibitor. *Mol Immunol.*

573   2008;45(16):4057-63.

574   11.   Beinrohr L, Harmat V, Dobo J, Lorincz Z, Gal P, and Zavodszky P. C1 inhibitor serpin

575   domain structure reveals the likely mechanism of heparin potentiation and

576   conformational disease. *J Biol Chem.* 2007;282(29):21100-9.

577   12.   Cummings RD. *Encyclopedic Reference of Genomics and Proteomics in Molecular*

578   *Medicine* Berlin, Heidelberg: Springer; 2005:704–18.

579   13.   Bause E. Structural requirements of N-glycosylation of proteins. Studies with proline

580   peptides as conformational probes. *Biochem J.* 1983;209(2):331-6.

581   14.   Stavenhagen K, Kayili HM, Holst S, Koeleman CAM, Engel R, Wouters D, et al. N- and

582   O-glycosylation analysis of human C1-inhibitor reveals extensive mucin-type O-

583   glycosylation. *Mol Cell Proteomics.* 2018;17(6):1225-38.

584   15.   Helenius A, and Aebi M. Intracellular functions of N-linked glycans. *Science.*

585   2001;291(5512):2364-9.

586   16.   Eldering E, Huijbregts CC, Lubbers YT, Longstaff C, and Hack CE. Characterization of

587   recombinant C1 inhibitor P1 variants. *J Biol Chem.* 1992;267(10):7013-20.

588   17.   Valderrama-Rincon JD, Fisher AC, Merritt JH, Fan YY, Reading CA, Chhiba K, et al. An

589   engineered eukaryotic protein glycosylation pathway in Escherichia coli. *Nat Chem Biol.*

590   2012;8(5):434-6.

591   18.   Lowenthal MS, Davis KS, Formolo T, Kilpatrick LE, and Phinney KW. Identification of

592   novel N-glycosylation sites at noncanonical protein consensus motifs. *J Proteome Res.*

593   2016;15(7):2087-101.

594   19.   Lizak C, Gerber S, Numao S, Aebi M, and Locher KP. X-ray structure of a bacterial

595   oligosaccharyltransferase. *Nature.* 2011;474(7351):350-5.

596   20.   Ren Z, Perkins SJ, Love-Gregory L, Atkinson JP, and Java A. Clinicopathologic

597   Implications of Complement Genetic Variants in Kidney Transplantation. *Front Med*

598   *(Lausanne).* 2021;8:775280.

599   21.   Joseph K, Bains S, Tholanikunnel BG, Bygum A, Aabom A, Koch C, et al. A novel assay

600   to diagnose hereditary angioedema utilizing inhibition of bradykinin-forming enzymes.

601   *Allergy.* 2015;70(1):115-9.

602   22.   Kajdacsi E, Jandrasics Z, Veszeli N, Mako V, Koncz A, Gulyas D, et al. Patterns of C1-

603   Inhibitor/Plasma Serine Protease Complexes in Healthy Humans and in Hereditary

604   Angioedema Patients. *Front Immunol.* 2020;11:794.

605   23.   Gosswein T, Kocot A, Emmert G, Kreuz W, Martinez-Saguer I, Aygoren-Pursun E, et al.

606   Mutational spectrum of the C1INH (SERPING1) gene in patients with hereditary

607   angioedema. *Cytogenet Genome Res.* 2008;121(3-4):181-8.

608   24.   Guryanova I, Suffritti C, Parolin D, Zanichelli A, Ishchanka N, Polyakova E, et al.

609   Hereditary angioedema due to C1 inhibitor deficiency in Belarus: epidemiology, access

610   to diagnosis and seven novel mutations in SERPING1 gene. *Clin Mol Allergy.*

611   2021;19(1):3.

612   25.   Nita-Lazar M, Wacker M, Schegg B, Amber S, and Aebi M. The N-X-S/T consensus

613   sequence is required but not sufficient for bacterial N-linked protein glycosylation.

614   *Glycobiology.* 2005;15(4):361-7.

615   26.   Förster T. *Natural Science.* The Bavarian Julius-Maximilians University of Wurzburg;

616   2006:114.

617   27.   Shrimal S, Cherepanova NA, and Gilmore R. Cotranslational and posttranslocational N-

618   glycosylation of proteins in the endoplasmic reticulum. *Semin Cell Dev Biol.* 2015;41:71-

619   8.

620   28.   Imai K, and Mitaku S. Mechanisms of secondary structure breakers in soluble proteins.

621   *Biophysics (Nagoya-shi).* 2005;1:55-65.

622   29.   Bordo D, and Argos P. Suggestions for "safe" residue substitutions in site-directed

623   mutagenesis. *J Mol Biol.* 1991;217(4):721-9.

624   30.   Bissler JJ, Cicardi M, Donaldson VH, Gatenby PA, Rosen FS, Sheffer AL, et al. A

625   cluster of mutations within a short triplet repeat in the C1 inhibitor gene. *Proc Natl Acad*

626   *Sci U S A.* 1994;91(20):9622-5.

627   31.   Grivceva-Panovska V, Kosnik M, Korosec P, Andrejevic S, Karadza-Lapic L, and

628   Rijavec M. Hereditary angioedema due to C1-inhibitor deficiency in Macedonia: clinical

629   characteristics, novel SERPING1 mutations and genetic factors modifying the clinical

630   phenotype. *Ann Med.* 2018;50(3):269-76.

631   32.   Loules G, Zamanakou M, Parsopoulou F, Vatsiou S, Psarros F, Csuka D, et al. Targeted

632   next-generation sequencing for the molecular diagnosis of hereditary angioedema due

633   to C1-inhibitor deficiency. *Gene.* 2018;667:76-82.

634   33.   Verpy E, Biasotto M, Brai M, Misiano G, Meo T, and Tosi M. Exhaustive mutation

635   scanning by fluorescence-assisted mismatch analysis discloses new genotype-

636   phenotype correlations in angioedema. *Am J Hum Genet.* 1996;59(2):308-19.

637   34.   Loli-Ausejo D, Lopez-Lera A, Drouet C, Lluncor M, Phillips-Angles E, Pedrosa M, et al.

638   In search of an association between genotype and phenotype in hereditary angioedema

639   due to C1-INH deficiency. *Clin Rev Allergy Immunol.* 2021;61(1):1-14.

640   35.   Malaby HL, and Kobertz WR. Molecular determinants of co- and post-translational N-

641   glycosylation of type I transmembrane peptides. *Biochem J.* 2013;453(3):427-34.

642   36.   Sidrauski C, and Walter P. The transmembrane kinase Ire1p is a site-specific
643   endonuclease that initiates mRNA splicing in the unfolded protein response. *Cell.*
644   1997;90(6):1031-9.

645   37.   Malaby HL, and Kobertz WR. The middle X residue influences cotranslational N-
646   glycosylation consensus site skipping. *Biochemistry.* 2014;53(30):4884-93.

647   38.   Ruiz-Canada C, Kelleher DJ, and Gilmore R. Cotranslational and posttranslational N-
648   glycosylation of polypeptides by distinct mammalian OST isoforms. *Cell.*
649   2009;136(2):272-83.

650   39.   Adams CJ, Kopp MC, Larburu N, Nowak PR, and Ali MMU. Structure and molecular
651   mechanism of ER stress signaling by the unfolded protein response signal activator
652   IRE1. *Front Mol Biosci.* 2019;6:11.

653   40.   Molinari M. N-glycan structure dictates extension of protein folding or onset of disposal.
654   *Nat Chem Biol.* 2007;3(6):313-20.

655   41.   Haukedal H, and Freude KK. Implications of glycosylation in Alzheimer's disease. *Front*
656   *Neurosci.* 2020;14:625348.

657   42.   Shrimal S, and Gilmore R. Glycosylation of closely spaced acceptor sites in human
658   glycoproteins. *J Cell Sci.* 2013;126(Pt 23):5513-23.

659   43.   Bolt G, Kristensen C, and Steenstrup TD. Posttranslational N-glycosylation takes place
660   during the normal processing of human coagulation factor VII. *Glycobiology.*
661   2005;15(5):541-7.

662   44.   Rout PK, and Verma M. Post translational modifications of milk proteins in
663   geographically diverse goat breeds. *Sci Rep.* 2021;11(1):5619.

664   45.   van Doorn MB, Burggraaf J, van Dam T, Eerenberg A, Levi M, Hack CE, et al. A phase I
665   study of recombinant human C1 inhibitor in asymptomatic patients with hereditary
666   angioedema. *J Allergy Clin Immunol.* 2005;116(4):876-83.

667 46. Parad RB, Kramer J, Strunk RC, Rosen FS, and Davis AE, 3rd. Dysfunctional C1

668   inhibitor Ta: deletion of Lys-251 results in acquisition of an N-glycosylation site. *Proc*

669   *Natl Acad Sci U S A.* 1990;87(17):6786-90.

670 47. Ponard D, Gaboriaud C, Charignon D, Ghannam A, Wagenaar-Bos IGA, Roem D, et al.

671   SERPING1 mutation update: Mutation spectrum and C1 Inhibitor phenotypes. *Hum*

672   *Mutat.* 2020;41(1):38-57.

673 48. Shah CH, Princic N, Evans KA, and Schultz BG. Real-world changes in costs over time

674   among patients in the United States with hereditary angioedema on long-term

675   prophylaxis with lanadelumab. *J Med Econ.* 2023;26(1):871-7.

676 49. Duran-Romana R, Houben B, De Vleeschouwer M, Louros N, Wilson MP, Matthijs G, et

677   al. N-glycosylation as a eukaryotic protective mechanism against protein aggregation.

678   *Sci Adv.* 2024;10(5):eadk8173.

679 50. Eisenack TJ, and Trentini DB. Ending a bad start: Triggers and mechanisms of co-

680   translational protein degradation. *Front Mol Biosci.* 2022;9:1089825.

681 51. Sato T, Sako Y, Sho M, Momohara M, Suico MA, Shuto T, et al. STT3B-dependent

682   posttranslational N-glycosylation as a surveillance system for secretory protein. *Mol Cell.*

683   2012;47(1):99-110.

684

685

Figure legends

687

688 **Figure 1. Schematic representation of protein domains and N-glycan for C1-INH.** (**A**)

689 The N-terminal domain includes resides 23-134 (pink). The C-terminal SERPIN domain consists

690 of residues 135-500 (blue). Signal peptide (SP) contains 22 residues and is included in

691 the numbering. Branched symbols, N-glycosylation (n=7); black circles, verified O-glycosylation

692 sites (n=7); white circles, potential O-glycosylation sites (n=7). N-glycosylation sites in the

693 SERPIN domain are highlighted in red. Protease cleavage site, P1-P1′ highlighted in purple.

694 NTD, amino-terminal domain; CTD, carboxyl-terminal domain. (Adapted from *The Complement*

695 *Factsbook, Figure 23.1).* (**B**) Representation of the N-glycan structure on C1-INH. Based on a

696 mass spectrometry study, the majority of the N-glycans on N238, N253 and N352 are

697 biantennary, approximately 80%, with $HexNAc_4Hex_5NeuAc_2$ being the most abundant structure

698 (14). *, the N272 glycosylation site has not been confirmed by mass spectrometry.

699

700 **Figure 2. Illustration of key domains in C1-INH.** The reactive center loop (RCL) is in pink.

701 The regions involved in SERPIN function are labeled. The P15-P9 portion of the RCL, the hinge

702 domain, is highly conserved and facilitates the insertion of RCL into the β sheets A (SA). The

703 breach region lies on the top of SA, the initial insertion site of RCL. The shutter domain,

704 composed of S3A and S5A, is in the center of SA and facilitates the RCL insertion. The gate

705 region consists of strands 3 and 4 from β sheets C (S3C and S4C). N-glycosylation sites are

706 shown as blue spheres. The P1 and P′ are displayed in rainbowstick and are responsible for

707 trapping the target protease. Strands of central SA are in cyan. The two disulfide bridges are

708 labeled and colored in red. Protein structures used for modeling were obtained from the PDB

709 database (PDB: 5DU3). The Figure was generated using Pymol (3.0) and serves as a model for

710 structure analyses in Figures 4-7. NTD, amino-terminal domain; CTD, carboxyl-terminal

711 domain.

712 **Figure 3. Illustrations of N-glycans on the SERPIN domain in C1-INH and a C1s̄/C1-INH**

713 **complex.** (**A**) Molecular model of N-glycans on the SERPIN domain in C1-INH (PDB: 5DU3).

714 Molecular modeling was performed on the GlyCAM-Web tool, Glycoprotein Builder

715 (https://glycam.org). The N-linked glycan structure was generated based on mass spectrometry

716 results (14). The N-GlcNAc linkage conformation was based on the simulation generated from

717 Glycoprotein Builder. (**B**) Structure of a C1s̄/C1-INH complex (PDB: 8W18). The structure of

718 active C1s̄ is shown in a cartoon representation in rainbow. The RCL is in violet. The P1 R466

719 and P1′ T467 residues are displayed in rainbowstick and are responsible for trapping the C1s̄.

720 The disulfide bridges are labeled and colored in red. Recombinant C1s̄ harbors a S632A

721 mutation, making it catalytically inert (PDB: 8W18) (9). Figures were produced using PyMOL

722 (3.0)

723

724 **Figure 4. N238-glycosylation site variants.** (**A**) Western blot (**W**B) analysis of supernatants

725 from transfected wild type (WT) C1-INH and variant constructs of N238 under reducing

726 conditions. The recombinant expression of N238A and A239D is comparable to WT (see Table

727 1). The secretion of N238del is markedly decreased compared with that of WT. The consensus

728 sequence of N238- glycosylation NXS/T is highlighted in blue, orange and red. (**B**–**E**)

729 Functional analysis of N238 variants. (**B** and **D**) Absorbance is plotted against protein

730 concentration. (**C** and **E**) Relative absorbance (RA) is computed as the absorbance of the

731 variant divided by the absorbance of the WT at concentrations of 1 μg/ml, 500 ng/ml, 250

732 ng/ml and 125 ng/ml, respectively. For PKa binding, the P value for the percentage differences

733 of N238A and A239D compared to WT are 0.918 and 0.254, respectively. For FXIIa binding, the

734 P value for the percentage differences of N238A and A239D compared to WT are 0.05 and

735 0.358, respectively. Data represent three separate experiments with bars corresponding to

736 SEM. One-way ANOVA with Dunnett's multiple comparisons test was used. **F.** Structural

737   analysis of N238 (PDB: 5DU3). N238 is located on the surface of Helix E (hE). N238del results

738   in the disruption of the consensus sequence NXS, which is required for the attachment of N-

739   glycan. In the absence of glycosylation, N238del likely leads to protein misfolding.

740

741   **Figure 5. N352-glycosylation site variants.** (**A**) WB analysis of supernatants from transfected

742   WT C1-INH and variant constructs of N352 under reducing conditions. One representative

743   experiment of three is shown. Recombinant expression of N352A, N352S and S354G is

744   comparable to WT, whereas N352del, L353P and S354del are barely secreted. The secretion of

745   N352I was decreased (see Table 1). The consensus sequence of N352-glycosylation NXS/T is

746   highlighted in blue, orange and red. (**B**–**E**) Binding analysis of N352 glycosylation site variants.

747   (**B** and **D**) Representation of PKa and FXIIa binding of N352A, N352S, N352I and S354G

748   compared to WT. (**C** and **E**) N352I and S354G demonstrate impaired binding to both PKa and

749   FXIIa. N352S showed decreased binding to PKa but not to FXIIa. Data represents mean $\pm$ SEM

750   of 3 independent experiments. **$P < 0.01$, ***$P < 0.001$, ****$P < 0.0001$. One-way ANOVA

751   with Dunnett's multiple comparisons test was used. (**F**) Structural analysis of N352. N352 is

752   located in the loop connecting strands 2 and 3 in the β-sheet B (S2B and S3B), which is the

753   hydrophobic core of C1-INH. N352del disrupts the packing of hydrophobic core and leads to

754   protein misfolding. The substitution of L353P can cause structural disturbances by disrupting

755   hydrogen bridges and affecting the packing of the loop between S2A and S3A, thus leading to

756   protein misfolding. Hydrogen bond, yellow dash line.

757

758   **Figure 6. N253-glycosylation site variants.** (**A**) WB analysis of supernatants from transfected

759   WT and N253 variant constructs under reducing conditions. Recombinant expression of N253

760   variants is comparable to WT, see Table 1. N253A, N253del, N254del and S255G disrupt the

761   N-glycan attachment and lead to a slightly lower M_r protein compared with WT. The consensus

762   sequence of N253- glycosylation NXS/T is highlighted in blue, orange and red. It contains two

763   Ns in this sequence. (**B**) WB analysis of variants N254del and S255G before and after

764   treatment with glycosidases. Recombinant expression of N254del and S255G are comparable

765   to WT, but with a slightly lower M_r compared with WT (lane 1). After deglycosylation treatment,

766   WB demonstrates that N254del (lane 8), S255G (lane 9) and WT have the same M_r. Δ, post-

767   degylcosylation. (**C**–**F**) Functional analysis of the N253-glycosylation site variants. (**C** and **E**)

768   Absorbance is plotted against protein concentrations. (**D** and **F**) Binding affinity of N253-

769   glycosylation site variants with PKa and FXIIa compared to WT. The binding affinity of N253A,

770   N254A, S255del, S255G, S255T to PKa and FXIIa is comparable to WT. N253del and N254del

771   exhibit mildly impaired binding to PKa and FXIIa. Results shown are from 3 independent

772   experiments. Data represent mean ± SEM. Significances were calculated by 1-way ANOVA and

773   Dunnett's multiple comparisons, *P <0.05, ***P < 0.001, ****P < 0.0001. (**G**) Structural

774   analysis of N253. The structure of active C1-INH is shown in a cartoon representation (PDB:

775   5DU3). N253 locates in the loop connecting strand 1 in the β-sheet A and Helix F.

776
777   **Figure 7. N272-glycosylation site variants.** (**A**) WB analysis of supernatants from transfected

778   WT and N272 variant constructs under reducing conditions. Recombinant expression of

779   N271del (lane 3) and N272del (lane 5) is decreased. N271A, N272A, N272D, N271-2del,

780   K273del and S275del (lanes 2, 4, 6, 7, 8 and 9) have normal secretion comparable to WT (lane

781   1), see Table 1. N272-linked glycan site has an atypical N-glycosylation consensus sequence,

782   NNKIS. The peptide sequence of N272- glycosylation NNKIS is highlighted in blue, purple,

783   orange and red. (**B**) WB analysis of variants N272del and K273del before and after treatment

784   with glycosidases. Before treatment, K273del (lane 3) has a slightly higher M_r compared with

785   N272del (lane 2). After treatment, WB demonstrates that N272del (lane 5) and K273del (lane 6)

786   have the same M_r. Human purified C1-INH is used as a positive control (lane 7, before

787   treatment; lane 8, after treatment). Adopted from *Insights into the pathogenesis of hereditary*

788   *angioedema using genetic sequencing and recombinant protein expression analyses*, by Ren et

789   al. 2023 (6). Δ, post degylcosylation. (**C**–**F**) Functional analysis of the N272 glycosylation site

790   variants. (**C and E**) Absorbance is plotted against protein concentrations. (**D and F**)

791   Comparison of PKa and FXIIa binding between WT and N272 glycosylation site variants. The

792   binding affinity of N271A, N272A, N272D to PKa and FXIIa is comparable to WT, whereas

793   N271del, N272del, K273del and N271-N272del exhibit impaired binding activity to both

794   substrates. Interestingly, S275del exhibits a markedly decreased binding to PKa but not to

795   FXIIa. Data represent mean ± SEM of 3 separate experiments. ***P < 0.001, ****P < 0.0001.

796   One-way ANOVA with Dunnett's multiple comparisons test was used. (**G**) Structural analysis of

797   N272del and K273del. K273 is located in the loop immediately after hF. The deletion of K273

798   will affect the conformation of hF. K273del, previously reported, results in a new N-glycosylation

799   site in C1-INH (37). The N271 residue is shown in pink; N272 in blue sphere and K273 in

800   purple.

801
802   **Figure 8. N-glycosylation at N238, N253 and N352 in the endoplasmic reticulum (ER).**

803   (**A**) STT3A transfers the oligosaccharide to N238 and N352 (NXS) in the nascent protein chain

804   cotranslationally. STT3B transfers the oligosaccharide to the N253 sequon in a posttranslational

805   manner. (**B**) Misfolded N352del triggers the cotranslational protein degradation (50). (**C**) With

806   preserved protein structure, 253del, even without posttranslational modification, is able to pass

807   the quality control system and be transported out of the ER.

808

809   **Table legends**
810

811   **Table 1: N-glycosylation variants: expression and functional assessment.** Wild type (WT)

812   recombinant C1-INH concentration, 26.4 ± 3.0 µg/ml. Kallikrein (PKa), FXIIa and C1s̄ binding

813   are measured by ELISA. *P* values are computed by using two-sided independent sample T-

814   tests and comparing the results to those for WT. [§] PKa and FXIIa binding, >75% normal; 50-

815   70% marginally decreased; <50% decreased (21). [†] C1$\bar{s}$ binding >67%, normal; 41%–67%,

816   equivocal; <41%, abnormal (6, 22). Data represent mean $\pm$ SEM of 3 separate experiments. *P

817    $\leq$ 0.05, **P $\leq$ 0.01, ***P $\leq$ 0.001, ****P $\leq$ 0.0001. One-way ANOVA with Dunnett's multiple

818   comparisons test was used. [#], variants reported in HAE patients; N, no significant difference; N[‡],

819   increased expression; del, deletion; D, decreased; ND, not done; MD, marginally decreased.

820   SEM, standard error of the mean.

821   **Table 2. Clinical pathogenic implication of N-glycan variants in HAE patients**. The allele

822   frequency (AF) information is only reported for S255T, 0.0029%. ACMG, American College of

823   Medical Genetics; N, normal; D, decreased; ND, not detected; NA, not available; VUS, variant

824   of uncertain significance.

825

N-glycosylation Sequon	Variants Reported	Mutagenesis	Expression	Recombinant Secretion (µg/ml), mean ± SEM	Kallikrein (PKa) Binding	FXIIa Binding§	C1s̄ Binding†
<u>N238</u>AS	A239D	N238A	N	29.2 ± 1.7	N	N	N (89.9% ± 1.7)
		N238del	D****	ND	ND	ND	ND
		A239D	N‡	34.0 ± 3.5	N‡	N	N (89.0% ± 1.3)
		S240del	D****	2.3 ± 0.5	ND	ND	D (13.3% ± 6.6)
<u>N352</u>LS	N352I# N352S L353P# S354G	N352A	N	21.6 ± 0.3	N	N	N (76.7 ± 2.7%)
		N352del	D****	0.32 ± 0.13	ND	ND	ND
		N352I#	D***	8.6 ± 1.6	D**	D****	N (78.0 ± 1.6%)
		N352S	N	30.7 ± 3.7	D**	N	N (82.3 ± 1.1%)
		S354del	D****	1.1 ± 0.2	ND	ND	ND
		L353P#	D****	ND	ND	ND	ND
		S354G	N	16.6 ± 1.3	D***	D****	N (86.6 ± 2.3%)
<u>N253</u>NS	S255G S255T #	N253A	N	24.6 ± 4.7	N	N	N (86.2 ± 0.1%)
		N253del	N‡	38.9 ± 2.8	MD*	D***	N (83.7 ± 2.7%)
		N254A	N	32.9 ± 1.8	N	N	N (86.1 ± 3.0%)
		N254del	N	30.4 ± 0.5	D****	D****	N (86.0 ± 1.4%)
		S255del	N	25.3 ± 0.4	N	N	N (88.8 ± 0.7%)
		S255G	N	22.4 ± 3.2	N	N	N (86.0 ± 3.7%)
		S255T #	N	20.0 ± 4.0	N	N	N (89.1 ± 1.1%)
<u>NN272</u>KIS	N272D N272del# N271-N272del# K273del#	N271A	N	22.3 ± 5.4	N	N	N (88.5 ± 5.7%)
		N271del	D***	8.3 ± 1.2	D****	D****	D (56.0 ± 7.9%)
		N272A	N	24.9 ± 4.2	N	N	N (83.0 ± 0.6%)
		N272del#	MD*	13.0 ± 1.2	D****	D****	D (51.3 ± 4.7%)
		N272D	N	24.0 ± 2.9	N	N	N (80.2 ± 2.4%)
		N271-N272del#	N	28.9 ± 1.6	D****	D****	D (29.6 ± 0.3%)
		K273del#	N	21.8 ± 3.2	D****	D****	D (36.4± 2.7%)
		S275del	N	28.1 ± 3.0	D****	MD***	N (68.4 ± 3.9%)

Table 1: N-glycosylation variants: expression and functional assessment. Wild type (WT) recombinant C1-INH concentration, 26.4 ± 3.0 µg/ml. Kallikrein (PKa), FXIIa and C1s̄ binding are measured by ELISA. *P* values are computed by using two-sided independent sample T-tests and comparing the results to those for WT. §PKa and FXIIa binding, >75% normal; 50-70% marginally decreased; <50% decreased (21). †C1s̄ binding >67%, normal; 41%–67%, equivocal; <41%, abnormal (6, 22). Data represent mean ± SEM of 3 separate experiments. *P ≤ 0.05, **P ≤ 0.01, ***P ≤ 0.001, ****P ≤ 0.0001. One-way ANOVA with Dunnett's multiple comparisons test was used. #, variants reported in HAE patients; N, no significant difference; N‡, increased expression; del, deletion; D, decreased; ND, not done; MD, marginally decreased. SEM, standard error of the mean.

N-glycosylation Site	Variants	Assessment		Classification		Family History	Clinical Summary
		Expression	Function	ACMG Interpretation	Modified Interpretation		
N253	S255T	N	N	VUS	Likely benign	NA	**N₂₅₃NS** sequon likely utilizes a posttranslational glycosylation mechanism. The replacement of S with T at S255 site theoretically should not affect the glycol attachment at the N253. As S255T demonstrates, it has preserved expression and function and is likely a benign missense variant.
N352	N352I	D	N	VUS	Likely pathogenic	NA	**N₃₅₂LS** sequon are likely required for cotranslational N-glycan modification. The disruption at N352 glycan attachment results in a decreased protein expression and functional defects. N352I results in expression defects and is likely causing HAE. L353P demonstrates abolished expression, leading to HAE.
	L353P	ND	ND	Pathogenic	Pathogenic	Yes	
N272	N272del	D	D	Pathogenic	Pathogenic	Yes	K273del gains an additional N-glycan at the **N₂₇₂IS** site, which leads to a dysfunctional protein. N271 and N272 positions are conserved among SERPINs (Supplemental Figure 1). The deletion of N271, N272 or both are deleterious.
	N271_ N272del	N	D	Likely pathogenic	Likely pathogenic	Yes	
	K273del	N	D	Likely pathogenic	Pathogenic	Yes	

837

838 **Table 2. Clinical pathogenic implication of N-glycan variants in HAE patients.** The allele
839 frequency (AF) information is only reported for S255T, 0.0029%. ACMG, American College of
840 Medical Genetics; N, normal; D, decreased; ND, not detected; NA, not available; VUS, variant
841 of uncertain significance.
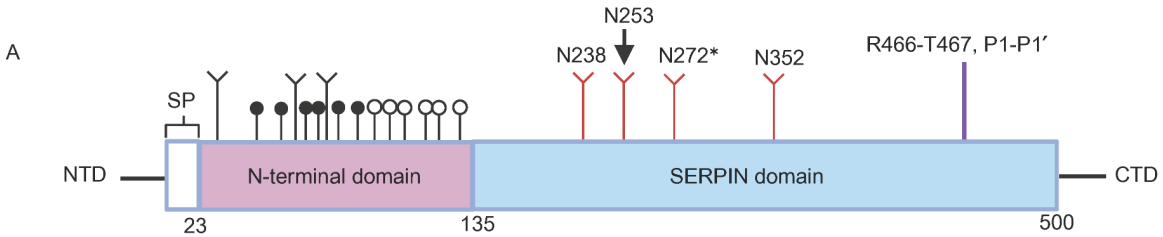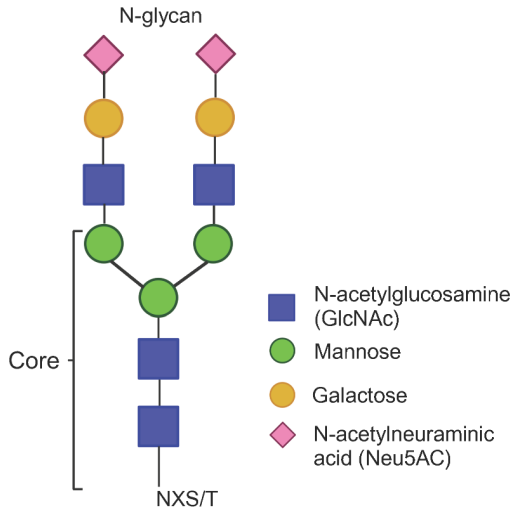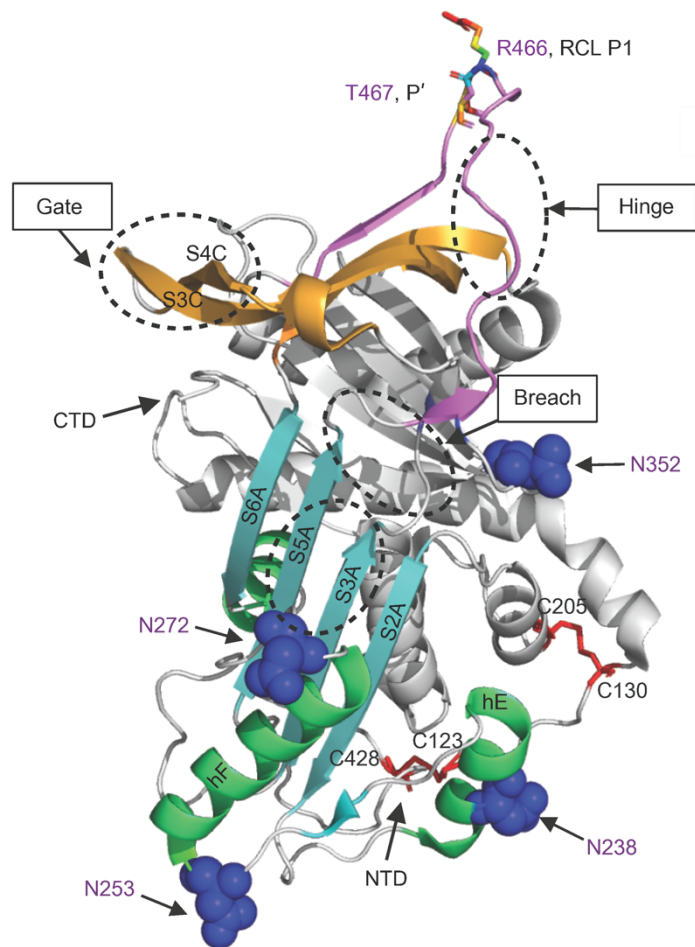
842

843

844

845

846

847

848

849

850

851

852

Figure 1. Schematic representation of protein domains and N-glycan for C1-INH. (**A**) The N-terminal domain includes resides 23-134 (pink). The C-terminal SERPIN domain consists of residues 135-500 (blue). Signal peptide (SP) contains 22 residues and is included in the numbering. Branched symbols, N-glycosylation (n=7); black circles, verified O-glycosylation sites (n=7); white circles, potential O-glycosylation sites (n=7). N-glycosylation sites in the SERPIN domain are highlighted in red. Protease cleavage site, P1-P1′ highlighted in purple. NTD, amino-terminal domain; CTD, carboxyl-terminal domain. (Adapted from *The Complement Factsbook, Figure 23.1).* (**B**) Representation of the N-glycan structure on C1-INH. Based on a mass spectrometry study, the majority of the N-glycans on N238, N253 and N352 are biantennary, approximately 80%, with $HexNAc_4Hex_5NeuAc_2$ being the most abundant structure (14). *, the N272 glycosylation site has not been confirmed by mass spectrometry.

864

Figure 2. Illustration of key domains in C1-INH. The reactive center loop (RCL) is in pink. The regions involved in SERPIN function are labeled. The P15-P9 portion of the RCL, the hinge domain, is highly conserved and facilitates the insertion of RCL into the β sheets A (SA). The breach region lies on the top of SA, the initial insertion site of RCL. The shutter domain, composed of S3A and S5A, is in the center of SA and facilitates the RCL insertion. The gate region consists of strands 3 and 4 from β sheets C (S3C and S4C). N-glycosylation sites are shown as blue spheres. The P1 and P' are displayed in rainbowstick and are responsible for trapping the target protease. Strands of central SA are in cyan. The two disulfide bridges are labeled and colored in red. Protein structures used for modeling were obtained from the PDB database (PDB: 5DU3). The Figure was generated using Pymol (3.0) and serves as a model for structure analyses in Figures 4-7. NTD, amino-terminal domain; CTD, carboxyl-terminal domain.

Figure 3. Illustrations of N-glycans on the SERPIN domain in C1-INH and a C1s̄/C1-INH complex. (**A**) Molecular model of N-glycans on the SERPIN domain in C1-INH (PDB: 5DU3). Molecular modeling was performed on the GlyCAM-Web tool, Glycoprotein Builder (https://glycam.org). The N-linked glycan structure was generated based on mass spectrometry results (14). The N-GlcNAc linkage conformation was based on the simulation generated from Glycoprotein Builder. (**B**) Structure of a C1s̄/C1-INH complex (PDB: 8W18). The structure of active C1s̄ is shown in a cartoon representation in rainbow. The RCL is in violet. The P1 R466 and P1′ T467 residues are displayed in rainbowstick and are responsible for trapping the C1s̄. The d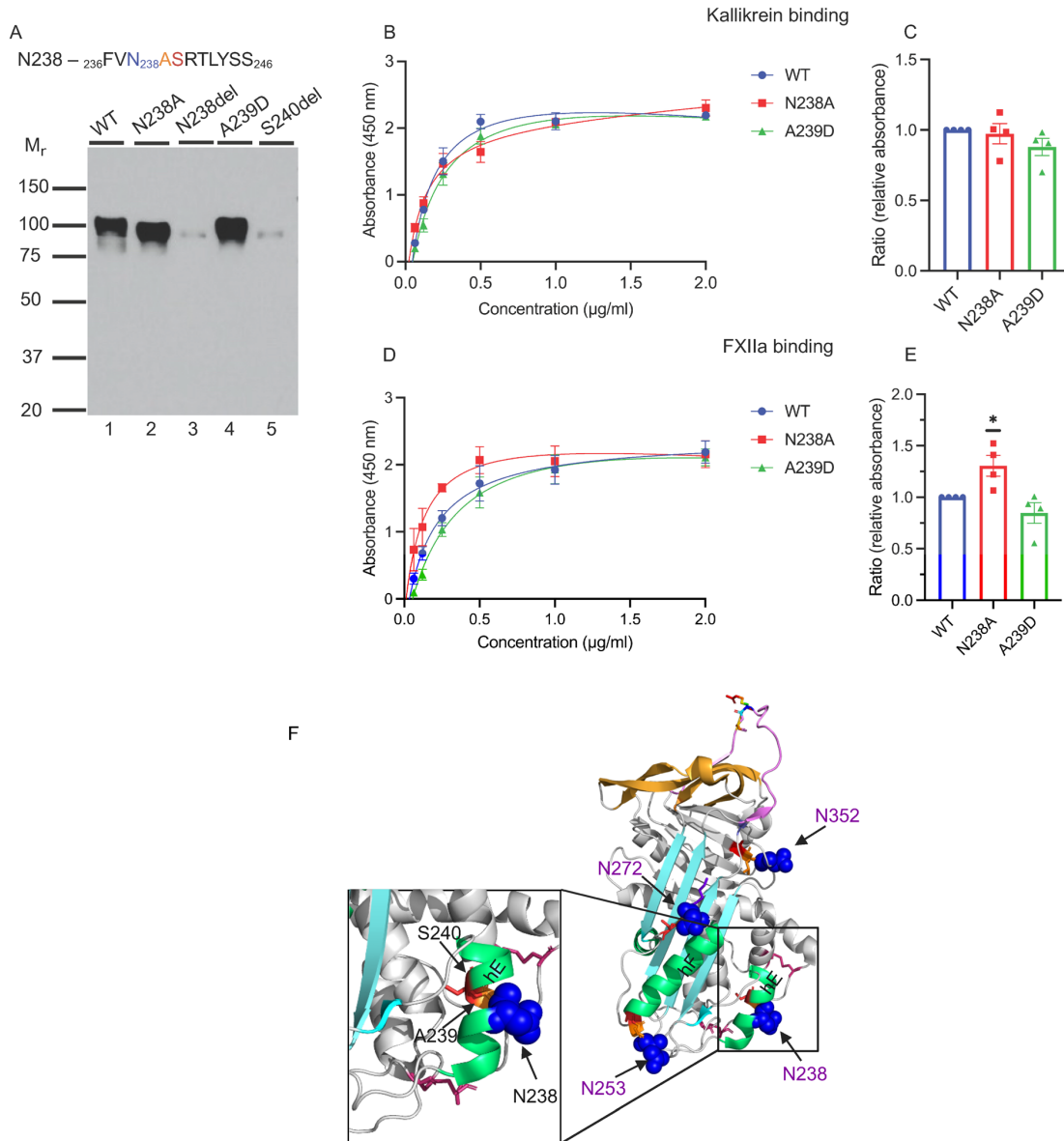isulfide bridges are labeled and colored in red. Recombinant C1s̄ harbors a S632A mutation, making it catalytically inert (PDB: 8W18) (9). Figures were produced using PyMOL (3.0)
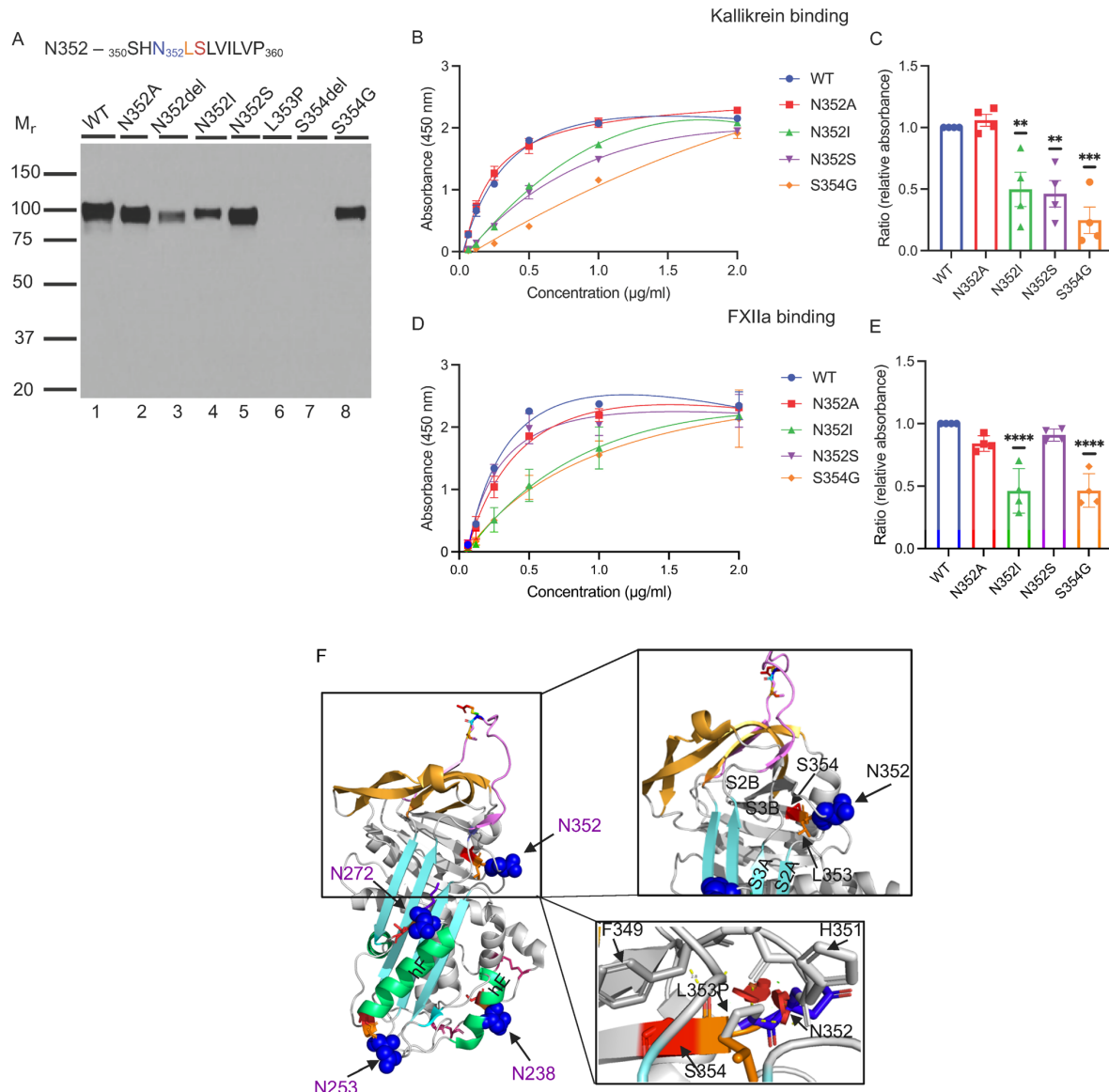
894

Figure 4. N238-glycosylation site variants. (**A**) Western blot **(**WB) analysis of supernatants

from transfected wild type (WT) C1-INH and variant constructs of N238 under reducing

conditions. The recombinant expression of N238A and A239D is comparable to WT (see Table

1). The secretion of N238del is markedly decreased compared with that of WT. The consensus

sequence of N238- glycosylation NXS/T is highlighted in blue, orange and red. (**B**–**E**)

Functional analysis of N238 variants. (**B** and **D**) Absorbance is plotted against protein

concentration. (**C** and **E)** Relative absorbance (RA) is computed as the absorbance of the

902   variant divided by the absorbance of the WT at concentrations of 1 μg/ml, 500 ng/ml, 250

903   ng/ml and 125 ng/ml, respectively. For PKa binding, the *P* value for the percentage differences

904   of N238A and A239D compared to WT are 0.918 and 0.254, respectively. For FXIIa binding, the

905   *P* value for the percentage differences of N238A and A239D compared to WT are 0.05 and

906   0.358, respectively. Data represent three separate experiments with bars corresponding to

907   SEM. One-way ANOVA with Dunnett's multiple comparisons test was used. **F.** Structural

908   analysis of N238 (PDB: 5DU3). N238 is located on the surface of Helix E (hE). N238del results

909   in the disruption of the consensus sequence NXS, which is required for the attachment of N-

910   glycan. In the absence of glycosylation, N238del likely leads to protein misfolding.

911

Figure 5. N352-glycosylation site variants. (**A**) WB analysis of supernatants from transfected WT C1-INH and variant constructs of N352 under reducing conditions. One representative experiment of three i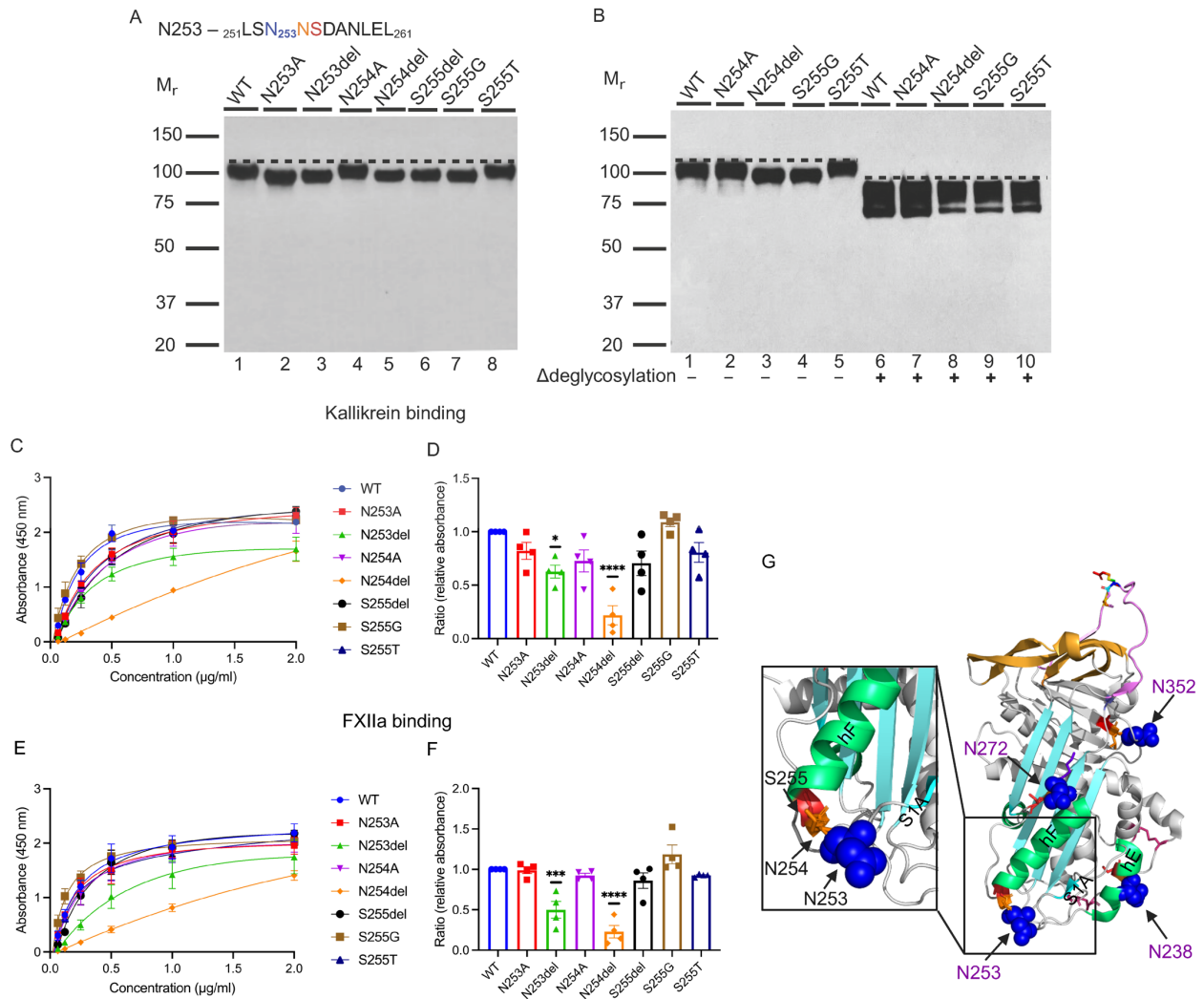s shown. Recombinant expression of N352A, N352S and S354G is comparable to WT, whereas N352del, L353P and S354del are barely secreted. The secretion of N352I was decreased (see Table 1). The consensus sequence of N352-glycosylation NXS/T is highlighted in blue, orange and red. (**B–E**) Binding analysis of N352 glycosylation site variants. (**B** and **D**) Representation of PKa and FXIIa binding of N352A, N352S, N352I and S354G
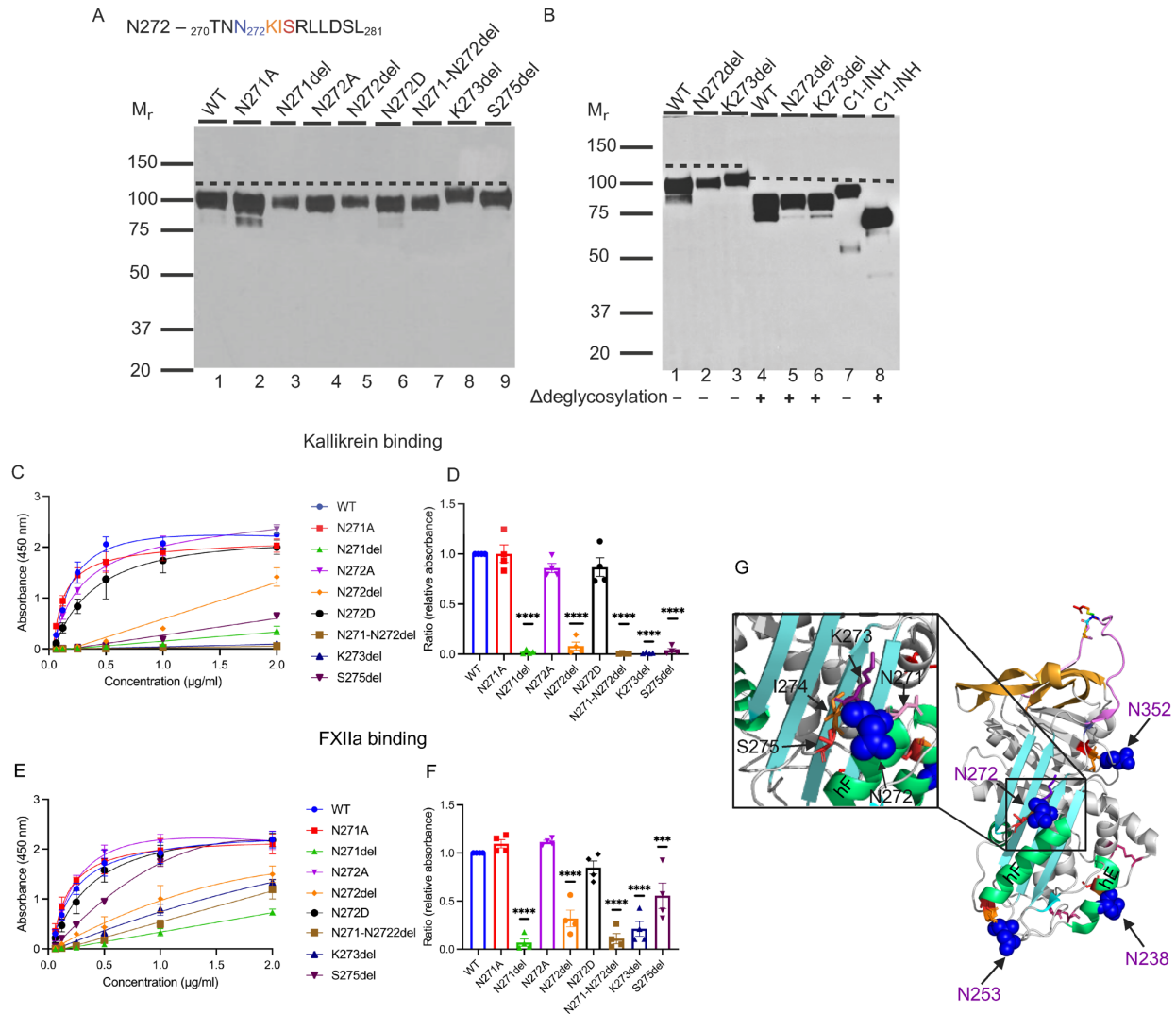
920   compared to WT. (**C** and **E**) N352I and S354G demonstrate impaired binding to both PKa and

921   FXIIa. N352S showed decreased binding to PKa but not to FXIIa. Data represents mean $\pm$ SEM

922   of 3 independent experiments. **$P < 0.01$, ***$P < 0.001$, ****$P < 0.0001$. One-way ANOVA

923   with Dunnett's multiple comparisons test was used. (**F**) Structural analysis of N352. N352 is

924   located in the loop connecting strands 2 and 3 in the β-sheet B (S2B and S3B), which is the

925   hydrophobic core of C1-INH. N352del disrupts the packing of hydrophobic core and leads to

926   protein misfolding. The substitution of L353P can cause structural disturbances by disrupting

927   hydrogen bridges and affecting the packing of the loop between S2A and S3A, thus leading to

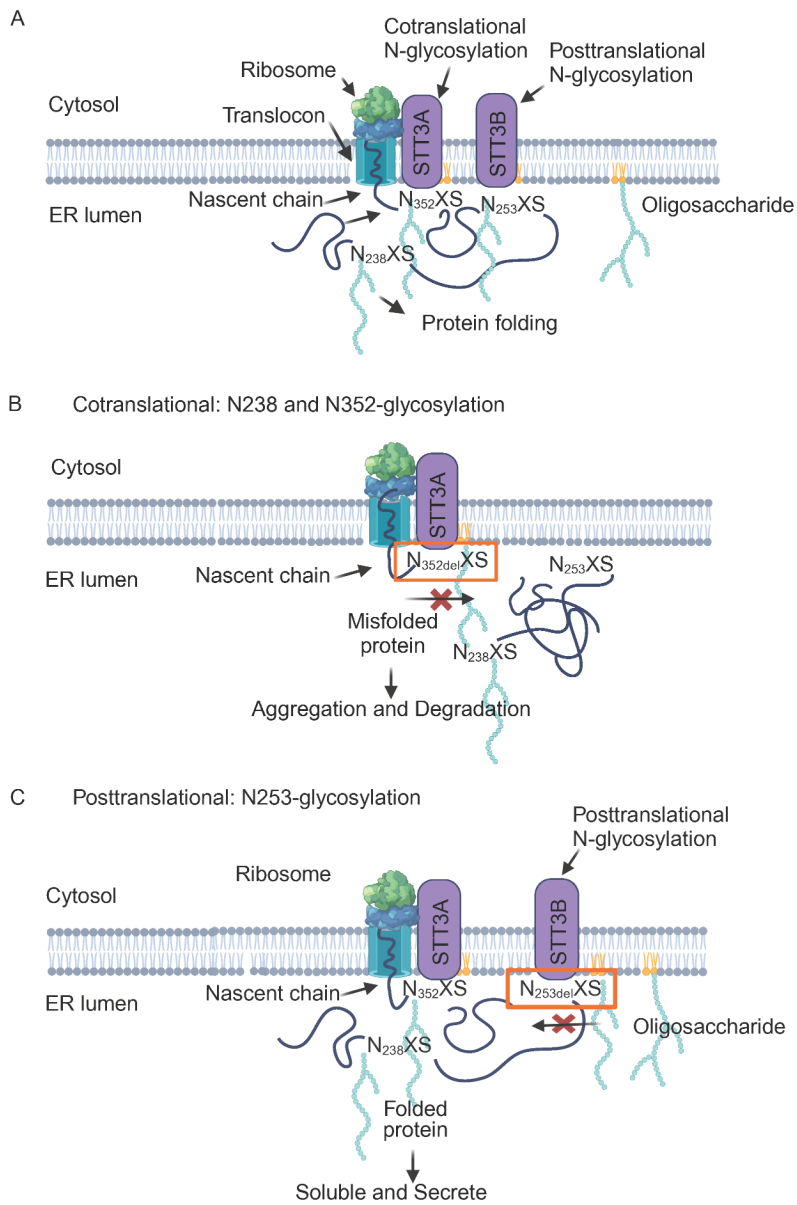928   protein misfolding. Hydrogen bond, yellow dash line.

Figure 6. N253-glycosylation site variants. (A) WB analysis of supernatants from transfected WT and N253 variant constructs under reducing conditions. Recombinant expression of N253 variants is comparable to WT, see Table 1. N253A, N253del, N254del and S255G disrupt the N-glycan attachment and lead to a slightly lower M_r protein compared with WT. The consensus sequence of N253- glycosylation NXS/T is highlighted in blue, orange and red. It contains two Ns in this sequence. (B) WB analysis of variants N254del and S255G before and after treatment with glycosidases. Recombinant expression of N254del and S255G are comparable

937 to WT, but with a slightly lower M_r compared with WT (lane 1). After deglycosylation treatment,

938 WB demonstrates that N254del (lane 8), S255G (lane 9) and WT have the same M_r. Δ, post-

939 degylcosylation. (**C**–**F**) Functional analysis of the N253-glycosylation site variants. (**C** and **E**)

940 Absorbance is plotted against protein concentrations. (**D** and **F**) Binding affinity of N253-

941 glycosylation site variants with PKa and FXIIa compared to WT. The binding affinity of N253A,

942 N254A, S255del, S255G, S255T to PKa and FXIIa is comparable to WT. N253del and N254del

943 exhibit mildly impaired binding to PKa and FXIIa. Results shown are from 3 independent

944 experiments. Data represent mean ± SEM. Significances were calculated by 1-way ANOVA and

945 Dunnett's multiple comparisons, *P <0.05, ***P < 0.001, ****P < 0.0001. (**G**) Structural

946 analysis of N253. The structure of active C1-INH is shown in a cartoon representation (PDB:

947 5DU3). N253 locates in the loop connecting strand 1 in the β-sheet A and Helix F.

Figure 7. N272-glycosylation site variants. (A) WB analysis of supernatants from transfected

WT and N272 variant constructs under reducing conditions. Recombinant expression of

N271del (lane 3) and N272del (lane 5) is decreased. N271A, N272A, N272D, N271-2del,

K273del and S275del (lanes 2, 4, 6, 7, 8 and 9) have normal secretion comparable to WT (lane

1), see Table 1. N272-linked glycan site has an atypical N-glycosylation consensus sequence,

NNKIS. The peptide sequence of N272- glycosylation NNKIS is highlighted in blue, purple,

orange and red. (B) WB analysis of variants N272del and K273del before and after treatment

with glycosidases. Before treatment, K273del (lane 3) has a slightly higher M_r compared with

957   N272del (lane 2). After treatment, WB demonstrates that N272del (lane 5) and K273del (lane 6)

958   have the same M_r. Human purified C1-INH is used as a positive control (lane 7, before

959   treatment; lane 8, after treatment). Adopted from *Insights into the pathogenesis of hereditary*

960   *angioedema using genetic sequencing and recombinant protein expression analyses*, by Ren et

961   al. 2023 (6). Δ, post degylcosylation. (**C**–**F**) Functional analysis of the N272 glycosylation site

962   variants. (**C and E**) Absorbance is plotted against protein concentrations. (**D and F**)

963   Comparison of PKa and FXIIa binding between WT and N272 glycosylation site variants. The

964   binding affinity of N271A, N272A, N272D to PKa and FXIIa is comparable to WT, whereas

965   N271del, N272del, K273del and N271-N272del exhibit impaired binding activity to both

966   substrates. Interestingly, S275del exhibits a markedly decreased binding to PKa but not to

967   FXIIa. Data represent mean $\pm$ SEM of 3 separate experiments. ***$P < 0.001$, ****$P < 0.0001$.

968   One-way ANOVA with Dunnett's multiple comparisons test was used. (**G**) Structural analysis of

969   N272del and K273del. K273 is located in the loop immediately after hF. The deletion of K273

970   will affect the conformation of hF. K273del, previously reported, results in a new N-glycosylation

971   site in C1-INH (37). The N271 residue is shown in pink; N272 in blue sphere and K273 in

972   purple.

Figure 8. N-glycosylation at N238, N253 and N352 in the endoplasmic reticulum (ER).

(**A**) STT3A transfers the oligosaccharide to N238 and N352 (NXS) in the nascent protein chain cotranslationally. STT3B transfers the oligosaccharide to the N253 sequon in a posttranslational manner. (**B**) Misfolded N352del triggers the cotranslational protein degradation (50). (**C**) With preserved protein structure, 253del, even without posttranslational modification, is able to pass the quality control system and be transported out of the ER.